Preparation and Characterization of Magnesium Ferrite/ Magnetite Nanocomposite Based Antimicrobial Material

N.M. Deraz[1]* and Omar H. Abd-Elkader[2,3]

[1]Physical Chemistry Department, Laboratory of Surface Chemistry and Catalysis,
National Research Center, Dokki, Cairo, Egypt.
[2]Zoology Department, College of Science, King Saud University,
Riyadh 11451, Kingdom of Saudi Arabia.
[3]Electron Microscope and Thin Films Department, National Research Center (NRC),
El- Behooth Street, 12622, Giza, Egypt.

Nanocrystalline magnesium ferrite/magnetite composite has been prepared by combustion technique. Structural characterization has been performed by X-ray diffraction XRD). Formation of magnesium ferrite/magnetite composite has also been studied by using infrared (IR). The chemical composition and surface morphology of the as prepared material were determined using energy dispersive X-ray (EDX), scanning electron microscope (SEM) and transmission electron microscope (TEM) techniques. SEM and TEM show formation of nano- materials with sponge-like structure. The concentration of constituents, involved in the as synthesized material was determined by using EDX technique. In fact, it was found the concentration of Mg, Fe and O species changes from the uppermost surface layer to the bulk of the system studied. Finally, XRD measurements display formation of $MgFe_2O_4/Fe_3O_4$ composite. It is well known that iron oxide based nanomaterials have many potential applications in biology due to their significant magnetic properties.

Key words: XRD, IR, SEM, TEM, EDX, $MgFe_2O_4$, Fe_3O_4.

Nanomaterials have been studied to be likely candidates for antimicrobial agents due to their large surface area to volume. Increasing of the contact surface area of nanomaterials or nanoparticles with the microbe and /or bacteria brought about an increase of their antibacterial/ antimicrobial activities due to the broad range of reactions with the bacterial and/microbial surface[1]. The resistance of microbes against nanoparticles is very low because these microbes require the microorganism to simultaneously undergo a series of mutations in order to protect themselves[2]. Metal oxide based nanoparticles have very important applications in different fields such as water treatment, cosmetics, medicine and catalysis[3]. The incorporation of antimicrobial metals into paints and fibers resulted in immense industrial and/or home applications.

Spinel materials such as Fe_3O_4 and ferrites are technologically important materials for data storage, transmission and biological applications due to their optical, electrical, magnetic, mechanical and catalytic properties[4]. Magnesium ferrite is one of the most important ferrites with a cubic structure of normal spinel-type. It is a soft magnetic n-type semiconducting material. This ferrite exhibits low saturation magnetization, high resistivity and uniform and reproducible characteristics[5].

Unique interactions of silver nanoparticles with microorganisms at nanoscale were occurred due to their unusual physical, chemical and biological properties[6]. Incorporation of silver nanoparticles in different materials has

---
* To whom all correspondence should be addressed.
E-mail: nmderaz@yahoo.com

been used in antibacterial applications. The antibacterial effects of silver doped zeolite / acrylonitryl polymer composite were studied to be used in computer parts such as keyboards and mouse-buttons. The antibacterial efficacy of these composites increases as the amount of silver increases to a certain limit[6].

Iron oxides based nanoparticles have many potential applications in biology due to their significant magnetic properties[7]. *Staphylococcus aureus* (PTCC 1431), *Escherichia coli* (PTCC 1395), *Pseudomonas aeruginosa* (PTCC 1599) and *Candida albicans* (PTCC 5027) were grown in the presence of both pure iron oxides (Fe_2O_3 and Fe_3O_4) nanoparticles and that incorporated in starch as dispersing agent in order to reinforce the colloidal stability of these oxides. The results reported that Fe_2O_3/starch nanocomposite did not inhibit microbial growth even at the highest concentration of Fe_2O_3 nanoparticles. But pure Fe_3O_4 nanoparticles and Fe_3O_4/starch nanocomposite inhibited microorganism's growth, especially at the highest concentration magnetite. However, the antimicrobial effects of Fe_3O_4/starch nanocomposite are greater than that of pure Fe_3O_4 nanoparticles[7].

$MgFe_2O_4$ nanoparticles were synthesized by combustion method using different amounts of glycine as fuel[8]. The change in the fuel content led to a significant effects in the structural, morphological and magnetic properties of the as prepared magnesium ferrite. The results showed that the as-prepared Mg ferrite nano-particles have the nanometer size and partially inverse spinel structure. The magnetic properties of Mg ferrite nano-particles depend upon their size and crystallinity. The maximum value of the saturation magnetization for the as-prepared Mg ferrite nano-particles was 32.85 emu/g due to increase of the particle size. Similar results were observed in case of hematite/maghemite nano-particles that synthesized by the same route[9].

The goal of this research is to prepare magnesium ferrite/magnetite nanocomposite using the glycine-assisted combustion method. The structural, spectroscopic and morphological properties of $MgFe_2O_4$/Fe_3O_4 nanocomposite were studied. In this study, the employed techniques are XRD, IR, SEM, TEM and EDX.

MATERIALS AND METHODS

Iron/magnesium mixed oxides was prepared by mixing calculated proportions of iron and magnesium nitrates with a certain amount of glycine. The mixed precursors were concentrated in a porcelain crucible on a hot plate at 400 ºC for quarter hour. The crystal water was gradually vaporized during heating and when a crucible temperature was reached, a great deal of foams produced and spark appeared at one corner which spread through the mass, yielding a voluminous and fluffy product in the container. The final product is milled by a gate mortar for different uses. The chemicals employed in the present work were of analytical grade supplied by Prolabo Company.

Techniques

An X-ray measurement of various mixed solids was carried out using a BRUKER D8 advance diffractometer (Germany). The patterns were run with Cu K radiation at 40 kV and 40 mA with scanning speed in 2 of 2 ° min[-1].

The crystallite size of both $MgFe_2O_4$ and Fe_3O_4 present in the investigated solids was based on X-ray diffraction line broadening and calculated by using Scherrer equation[10].

$$d = \frac{B\lambda}{\beta \cos\theta}$$

where d is the average crystallite size of the phase under investigation, B is the Scherrer constant (0.89), λ is the wave length of X-ray beam used, is the full-width half maximum (FWHM) of diffraction and is the Bragg's angle.

An infrared transmission spectrum of various solids was determined using Perkin-Elmer Spectrophotometer (type 1430). The IR spectra were determined from 4000 to 400 cm^{-1}. Two mg of each solid sample were mixed with 200 mg of vacuum-dried IR-grade KBr. The mixture was dispersed by grinding for 3 min in a gate mortar and placed in a steel die 13 mm in diameter and subjected to a pressure of 5 tones. The sample disks were placed in the holder of the double grating IR spectrometer.

Scanning electron micrographs (SEM) were observed on SEM model JXA-840 electron microanalyzer. Transmission electron micrographs

(TEM) were recorded on TEM model EM10 Zeiss instrument. The samples were dispersed in ethanol and then treated ultrasonically in order disperse individual particles over a gold grids.
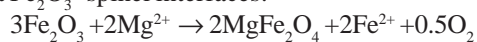
Energy dispersive X-ray analysis (EDX) was carried out on Hitachi S-800 electron microscope with an attached kevex Delta system. The parameters were as follows: accelerating voltage 15 kV, accumulation time 100s, window width 8 µm. The surface molar composition was determined by the Asa method, Zaf-correction, Gaussian approximation.

Table 1. The atomic abundance of elements measured at 20 keV and different points over the as prepared sample

Elements	Point 1	Point 2	Point 3
O	25.97	26.14	25.90
Mg	12.80	13.40	12.59
Fe	61.23	60.46	61.51

In previous work, one author suggested that Fe_2O_3 decomposes to $^2Fe_{2+}$ and oxygen gas at Fe_2O_3-spinel interface[8]. However, oxygen moves through the reacted area to be added to the spinel-MgO interface and form spinel by reacting with Fe^{2+} and MgO:
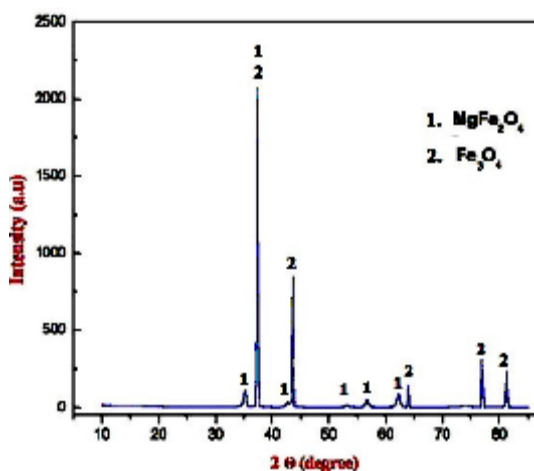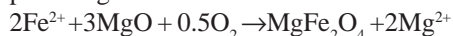
At Fe_2O_3- spinel interfaces:

$$3Fe_2O_3 +2Mg^{2+} \rightarrow 2MgFe_2O_4 +2Fe^{2+} +0.5O_2$$

At spinel-MgO interfaces:

$$2Fe^{2+} +3MgO + 0.5O_2 \rightarrow MgFe_2O_4 +2Mg^{2+}$$

RESULTS AND DISCUSSION

Fig. 1 showed XRD pattern for the as prepared sample which consisted entirely of nano-crystalline MgFe2O4 (minor phase) and Fe3O4 (major phase) with the Fd3m space group depending upon JCPDS cards No. 80-0072 and 26-1136, respectively. The Formation of magnesium ferrite depends upon substitution of ferrous ions involved in Fe_3O_4 by magnesium ions yielding $MgFe_2O_4$.

Table 2. The atomic abundance of elements measured at different applied voltages on the same point over the as prepared sample

Elements	10keV	15keV	20keV
O	30.05	27.70	26.49
Mg	26.92	18.79	14.60
Fe	43.03	53.52	58.91

An IR spectrum of the as prepared specimen was determined in the range of 4000 - 400 cm^{-1} as shown in Fig. 2. This figure showed that the as prepared sample has two main metal-oxygen bands indicating to the spinel structure[11]. The highest band locates at 556cm^{-1}, confirms an intrinsic stretching vibrations of metal at the tetrahedral site (Fe↔O), whereas the lowest band at 410 cm^{-1} displays octahedral- metal stretching (Mg↔O). The bands at 3470 cm^{-1}, 1637 cm^{-1} and

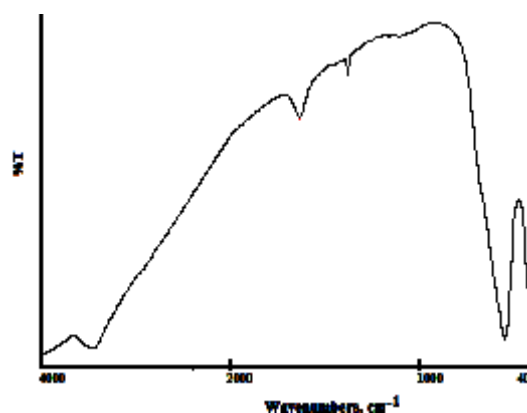**Fig. 1**. XRD pattern for the as prepared sample

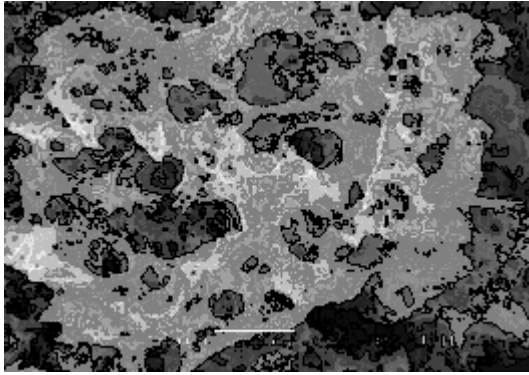**Fig. 2**. IR spectrum for the as prepared sample

Fig. 3. SEM image for the as prepared sample

1384 cm^{-1} are related to the stretching modes and H-O-H bending vibration of the free and/or absorbed water [12]. These observations confirm the formation of material with spinel structure[11].

The surface morphology of the as prepared sample was determined by scanning electron micrograph (SEM) as shown in Fig. 3. It can be seen from this figure that the as synthesized material is spongy with different voids and pores. Fig. 4a-b shows the transmission electron micrographs (TEM) for the as synthesized specimen with different magnification. TEM images
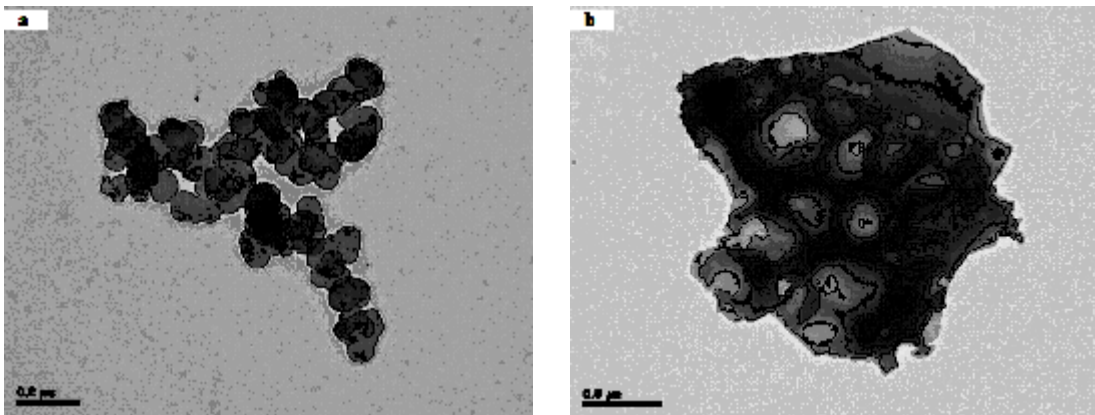

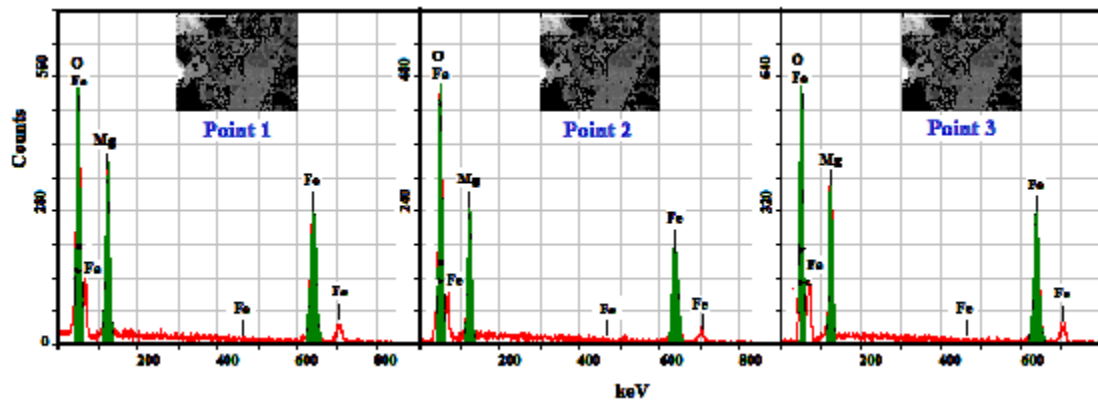**Fig. 4**. TEM image for the as prepared sample

Fig. 5. EDX pattern for the as prepared sample at different points and 20keV

display that the as prepared composite consisted of spherical particles. The particle size of the prepared composite ranged between 20nm and 30nm. This result confirms the crystallite sizes calculated by XRD technique.

Energy dispersive X-ray (EDX) technique

with different voltages and also different points on the surface of sample shows both the homogeneity and gradient of the elements involved in the sample. Figs. 5 and 6 show the EDX spectra at different points on the surface of sample and also at different applied voltages, respectively.
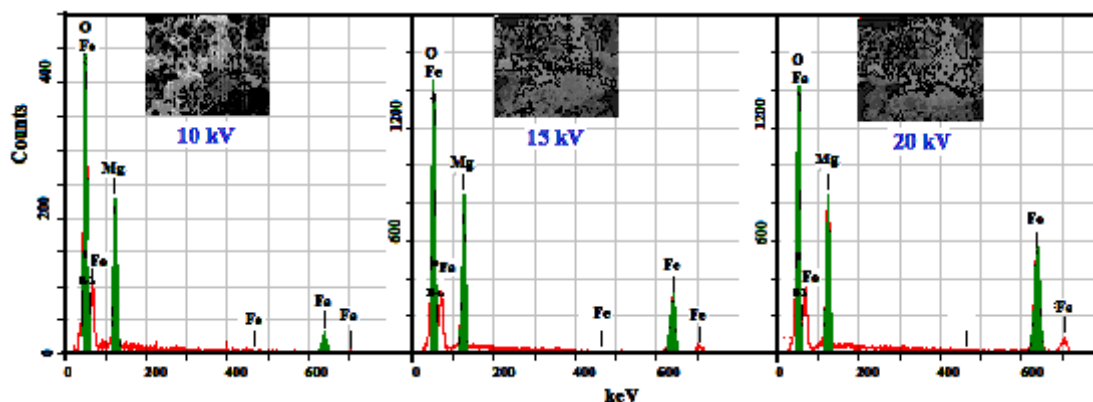
Fig. 6. EDX pattern for the as prepared sample at the same point with different applied voltages.

These figures showed that the as prepared sample has homogenous particles with gradual gradient of the elements involved in composite studied

The concentrations of various elements (O, Mg and Fe) involved in the investigated solid at 20 keV over different points on the sample surface are shown in Table 1. These concentrations are very close to each other indicating to the homogeneity of the as prepared system. In pure Fe_3O_4 compound iron content is 72.36%, thus the product purity can be calculated depending upon EDX data in Table 1. It was found that the purity of Fe_3O_4 is 84.62%. This result indicates that impurities exist corresponding to additional reflections related to $MgFe_2O_4$ as shown in Fig. 1.

The concentrations of O, Mg and Fe species from the uppermost surface to the bulk layers of the as prepared sample were determined using EDX technique at 10, 15 and 20 keV as shown in Table 2. This table showed that the concentrations of Mg and O species for the as prepared sample decreases as the applied voltage increases. The opposite behavior was observed in the case of Fe species.

CONCLUSIONS

Solid state reaction between MgO and Fe_2O_3 led to formation of Mg ferrite using various methods. One of these methods is glycine- assisted combustion method. In this study, this route resulted in formation spinel $MgFe_2O_4/ Fe_3O_4$ nanocomposite depending upon XRD and IR data. The particle size of the as prepared system display varies between 20nm and 30 nm. However, the liberation of different gases during preparation process brought about spongy and homogeneous material with spherical particles as shown in the SEM, TEM and EDX measurements. It is well known that iron oxide based nanomaterials have many potential applications in biology due to their significant magnetic properties[6, 8].

REFERENCES

1. Holister, P., Weener, J.W., Romas, Vas C., Harper, T., Nanoparticles: technology white papers 3. London: Cientific Ltd; 2003.
2. Pal S, Tak YK, Song JM. Does the antibacterial activity of silver nanoparticles depend on the shape of the nanoparticle? A study of the gram-negative bacterium Escherichia coli. *Applied Environmental Microbiology.* 2007; **73**:1712-1720.
3. Gupta, A.K., Gupta, M., Synthesis and surface engineering of iron oxide nanoparticles for biomedical applications. *Biomaterials.* 2005; **26**: 3995-4021.
4. Patil, K. C., Hegde, M. S., Rattan, T., Aruna S. T. , Chemistry of Nanocrystalline Oxide Materials, 1st ed., World Scientific Publishing Co. Pte. Ltd, Singapore. 2008, pp. 1-7.
5. Dogra, A., Singh, M., Kuma, R., *Nucl. Instr. and Meth.* 2003; **207**: 296-300.
6. Fahimdokht Mokhtari, F., Salahi, E., Ramesh Mehrpour, R., Asgari, M., Heidarpour, M.,

Shokrollahi, F., Antibacterial Effects of Polymers Impregnated by Nano Silver Manufactured as Computer Parts, *J.Pure Appl Microbiol*. 2013; **7**: 2213-2218.

7.   Zafari, M., Jafarpour, M., Biazar, E., Heidari, K. S., Antimicrobial Effects of Iron Oxide Nanoparticles in the Presence of Dispersing Agent, *J.Pure Appl Microbiol*, 2013; **7**: 143-149.

8.   Deraz, N., Alarifi, A., Novel preparation and properties of magnesioferrite nanoparticles, *J. Anal. Appl. Pyrolysis*. 2012; **97**: 55-61.

9.   Deraz, N., Alarifi, A., Novel processing and magnetic properties of hematite/maghemite nano-particles, *Ceramics International.* 2012; **38**: 4049-4055.

10.   Cullity, B. D., Elements of X-ray Diffraction, Addison-Wesly Publishing Co. Inc. 1976 (Chapter 14).

11.   Waldron, R. D., *Phys. Rev*. 1955; **99**: 1727-1735.

12.   Sankaranarayana, V.K.,   Sreekumar, C. , Precursor synthesis and microwave processing of nickel ferrite nanoparticles, *Curr. Appl. Phys*. 2003; **3**: 205-208.